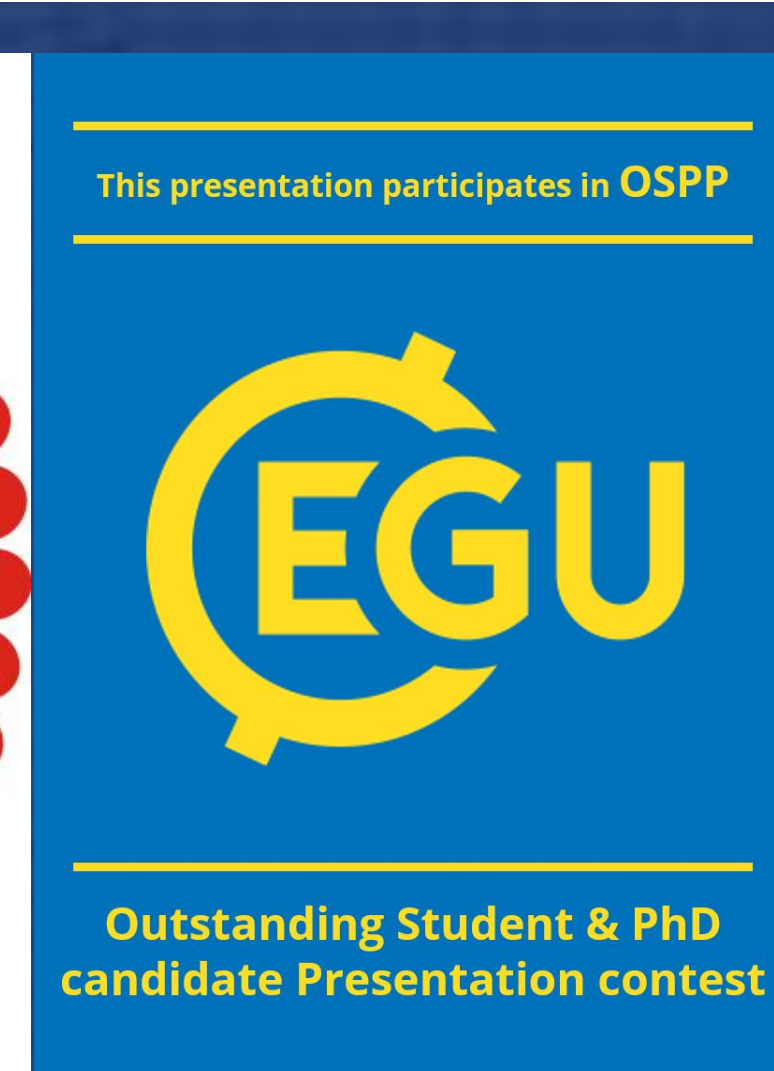
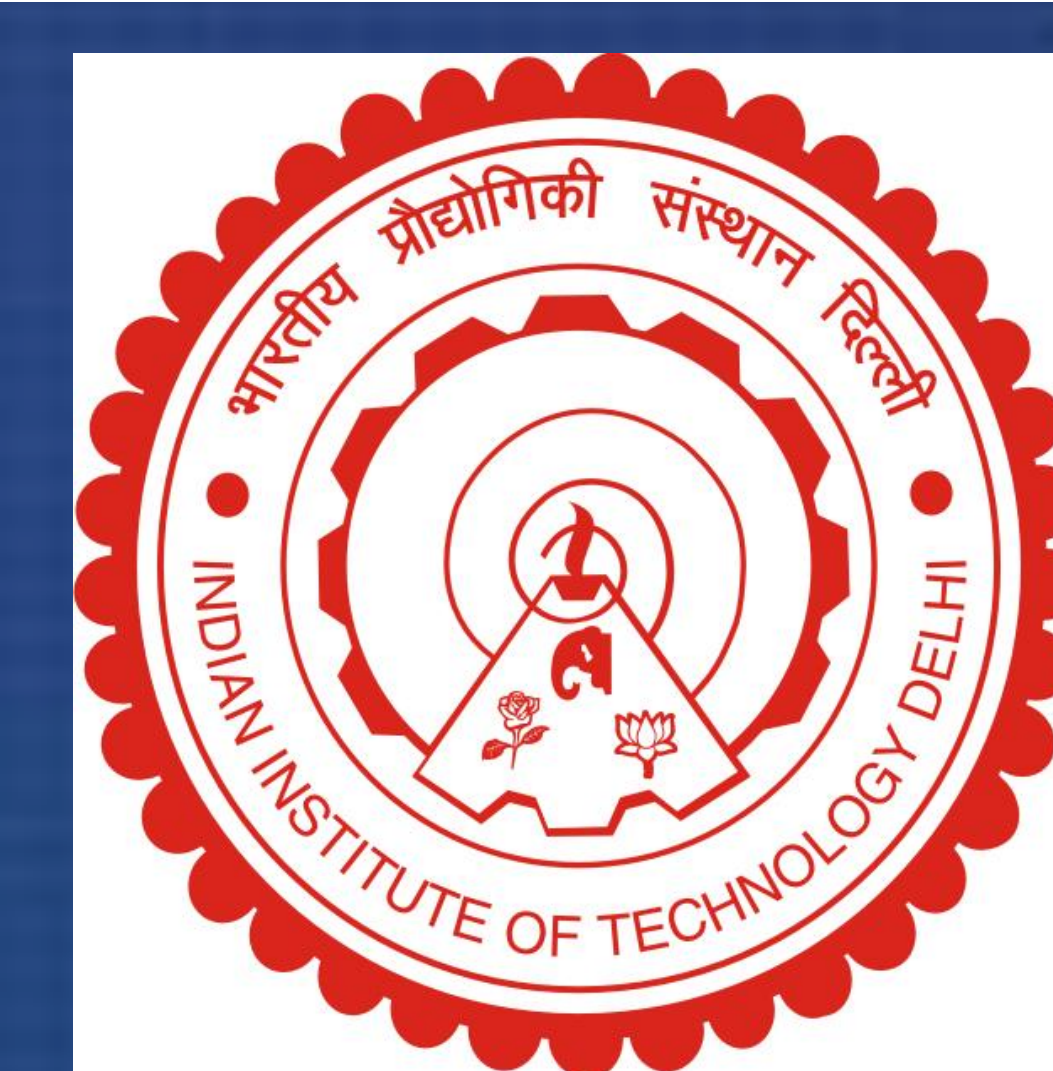




# Relationship of the predictability of North Pacific Mode and ENSO with predictability of PDO

Jivesh Dixit<sup>1</sup> and Krishna M. AchutaRao<sup>1</sup>

<sup>1</sup>Centre for Atmospheric Sciences, Indian Institute of Technology (IIT) Delhi  
Email: jiveshdixit@cas.iitd.ac.in, jiveshdixit@gmail.com



## Introduction and Motivation

Decadal Climate Variability (DCV) perturbs the regional climate across the globe at multi-year to decadal timescales. Various DCVs are hosted in Ocean basins due to coupling of Ocean and atmosphere. One such DCV mode, Pacific Decadal Oscillation (PDO) is defined as leading orthonormal mode of anomalous SST variability in the Pacific ocean. Despite being hosted in the fractional part of ocean, it influences the climate in various parts of the globe through atmospheric and oceanic teleconnections. *In the past centuries, a series of dry/wet epochs have been observed in various parts of the globe. Associated famines/floods have adversely affected the socio-economic interests of people living in those regions.* PDO, can aggravate uncertainty in ongoing human induced warming trend by redistributing heat content between surface and subsurface Ocean waters which in turn influences the regional climate.

Chen & Wallace (2016) analysed entire Pacific SST to obtain two leading orthogonal modes similar to Deser & Blackmon (1995). Two different linear combination of these modes resembles with dominant SST modes in Pacific i.e. PDO-like variability and ENSO-like variability.

Prediction of PDO at significant lead time can enable us predict regional climatic parameters of societal importance such as surface temperature, precipitation, humidity etc.

We hypothesize that the predictability of first two orthogonal modes of SST variability (20S-70N, 110E-90W: hereafter study region (SR)) influences the predictability of PDO mode as it can be defined as the linear combination of two linearly independent modes of SST variability.

## Data

For our analysis we have chosen Extended Reconstructed Sea Surface Temperature (ERSSTv5) dataset to represent observation and all the CMIP6 (Eyring *et al.*, 2016) models that participate in historical as well as in DCP-A (Boer *et al.*, 2016) hindcast experiments with 10 years temporal extent initialized every year starting from 1960.

CMIP6 Models / Observation	Hindcast ensembles	Historical ensembles	$\alpha$	$\beta$
BCC-CSM2-MR	8	1	0.17	0.97
CMCC-CM2-SR5	10	1	0.72	0.68
CanESM5	40	1	0.69	0.69
EC-Earth3 (i1, i2)	10, 5	1 (i1)	0.57	0.81
HadGEM3-GC31-MM	10	1	0.58	0.80
IPSL-CM6A-LR	10	1	0.43	0.88
MIROC6	10	1	0.71	0.57
MPI-ESM1-2-HR	10	1	0.60	0.77
NorCPM1 (i1, i2)	10, 10	1 (i1)	0.37	0.92
ERSSTv5 (Observation)	-	-	0.71	0.71

Values of ' $\alpha$ ' and ' $\beta$ ' are for single realization in CMIP6 historical experiments, which is typical for all the ensemble members in the given model.

## Methodology

Model's ability to simulate two leading observed EOF patterns; Interannual mode (IAM) and NPM patterns and associated timescales is examined by comparing two leading orthogonal SST modes in SR.

$$Mode_{IAM+NPM} := \alpha \cdot Mode_{IAM} + \beta \cdot Mode_{NPM}$$

$$\alpha = \beta = \frac{1}{\sqrt{2}} \text{ (For ERSSTv5)}$$

$$\alpha \neq \beta \text{ (For CMIP6 Models)}$$

Furthermore, to assess the prediction skill of DCP-A hindcast experiments, we used the following deterministic performance metrics:

$$ACC = \frac{\sum_{i=1}^N (f_i - \bar{f})(o_i - \bar{o})}{\sqrt{\sum_{i=1}^N (f_i - \bar{f})^2} \sqrt{\sum_{i=1}^N (o_i - \bar{o})^2}}$$

$$persistence = \frac{Cov(Obs_{LY_1}, Obs_{LY_{t+1}})}{\sqrt{Var(Obs_{LY_1})} \sqrt{Var(Obs_{LY_{t+1}})}}$$

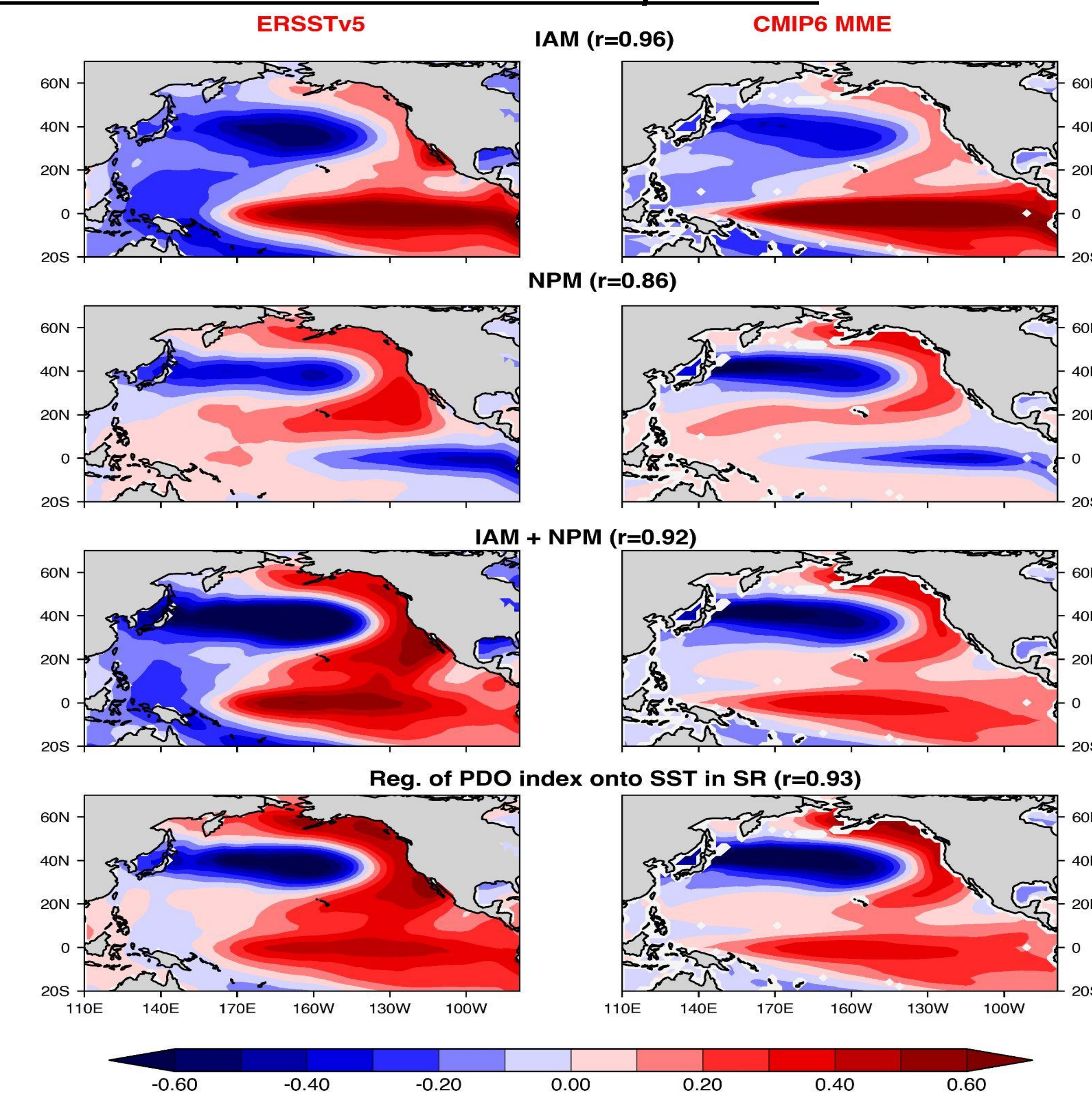
Area under the curve between "True positive rate" and "False positive rate" termed as ROC-AUC score and is used to assess the probabilistic skill of the model to predict the phase of the variability.

$$TPR = \frac{TP}{TP + FN}$$

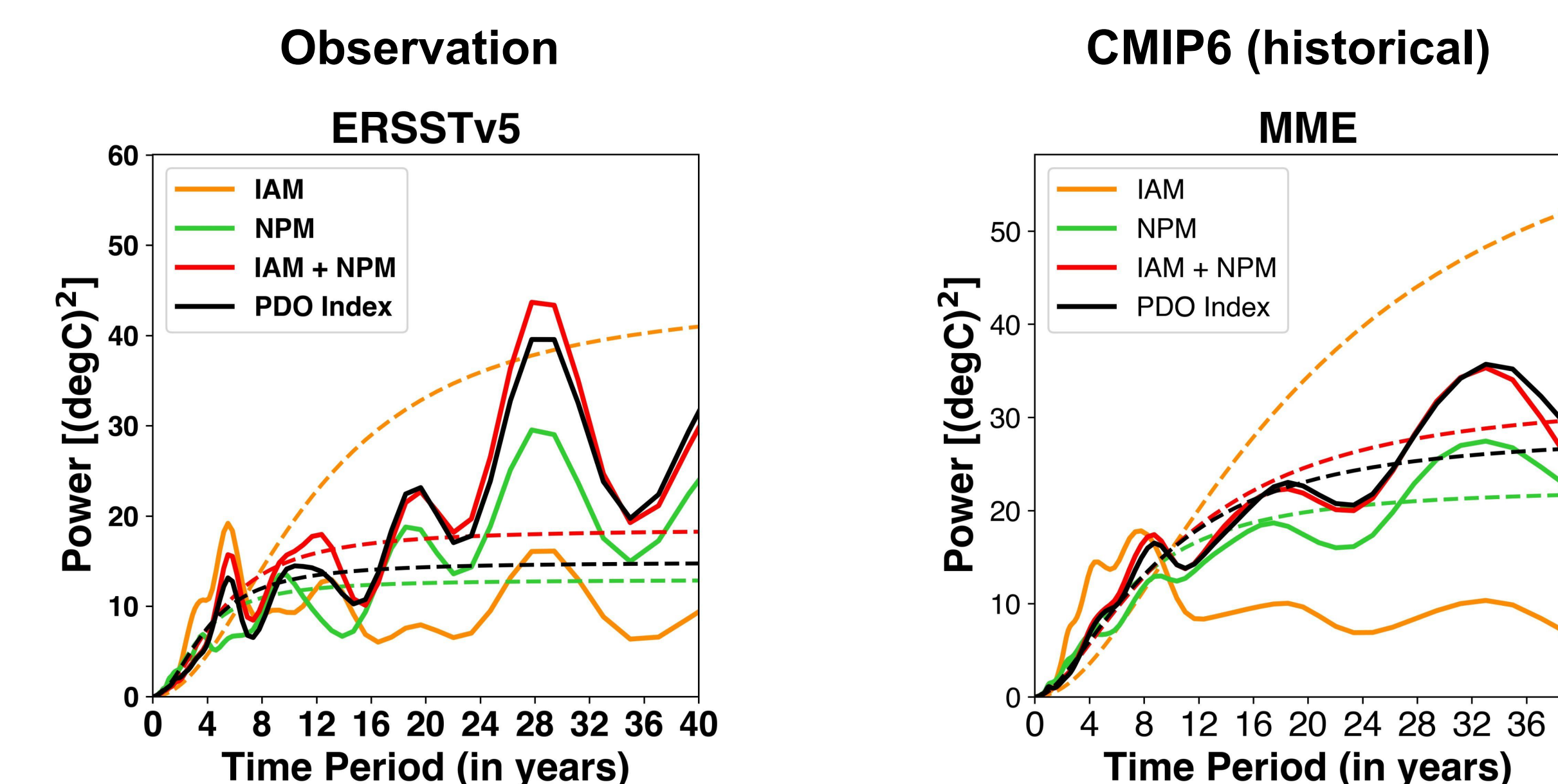
$$FPR = \frac{FP}{TN + FP}$$

## Results

### IAM and NPM modes in CMIP6 historical experiments:



Here ' $r$ ' represents the spatial correlation.  
Spatial correlation between "IAM+NPM" and "Regression of PDO index onto SST in SR" is 0.88 and 1 for MME and ERSSTv5 respectively.



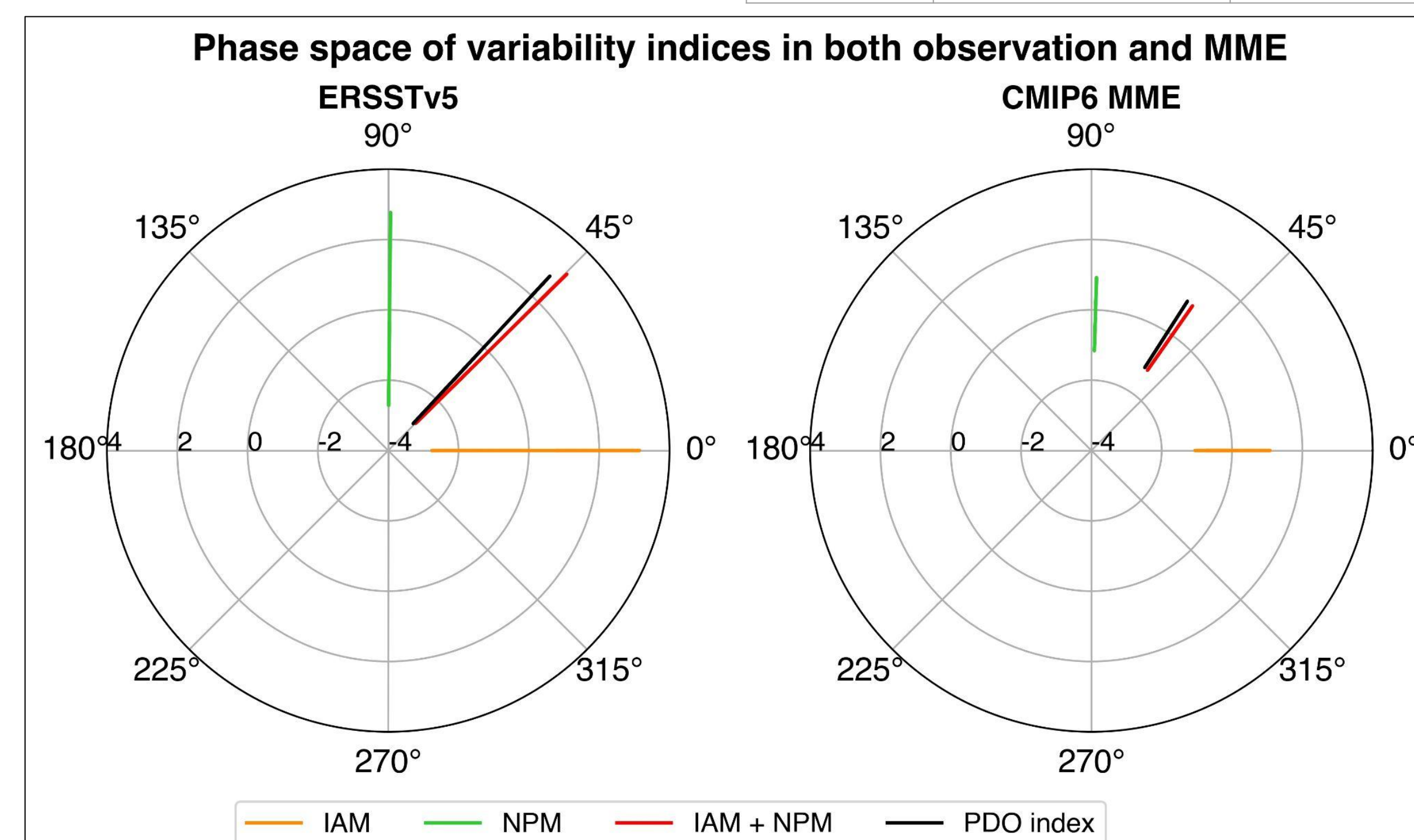
IAM is entirely interannual whereas NPM is entirely decadal mode of variability in both observations and MME.

PDO and "IAM + NPM" in CMIP6 MME doesn't show any observed interannual peak.

Observed spectral peak of 16-20 years in both "IAM + NPM" and PDO index is missing in CMIP6 MME.

Power spectra of "IAM + NPM" closely represents the power spectra of PDO in both MME and ERSSTv5.

Time Series	Spectral peaks (Obs)	Spectral peaks (MME)
IAM	4-8	4-8
NPM	8-12, 16-24, 24-32	28-36
IAM + NPM	4-8, 8-12, 16-20, 24-32	8, 28-36
PDO index	4-8, 8-12, 16-20, 24-32	8, 28-36



Length of the lines represent the amplitude of the variability, whereas angle between them represents the phase angle between the variability modes.

### Prediction skill of CMIP6 hindcast experiments to predict IAM, NPM and "IAM + NPM":

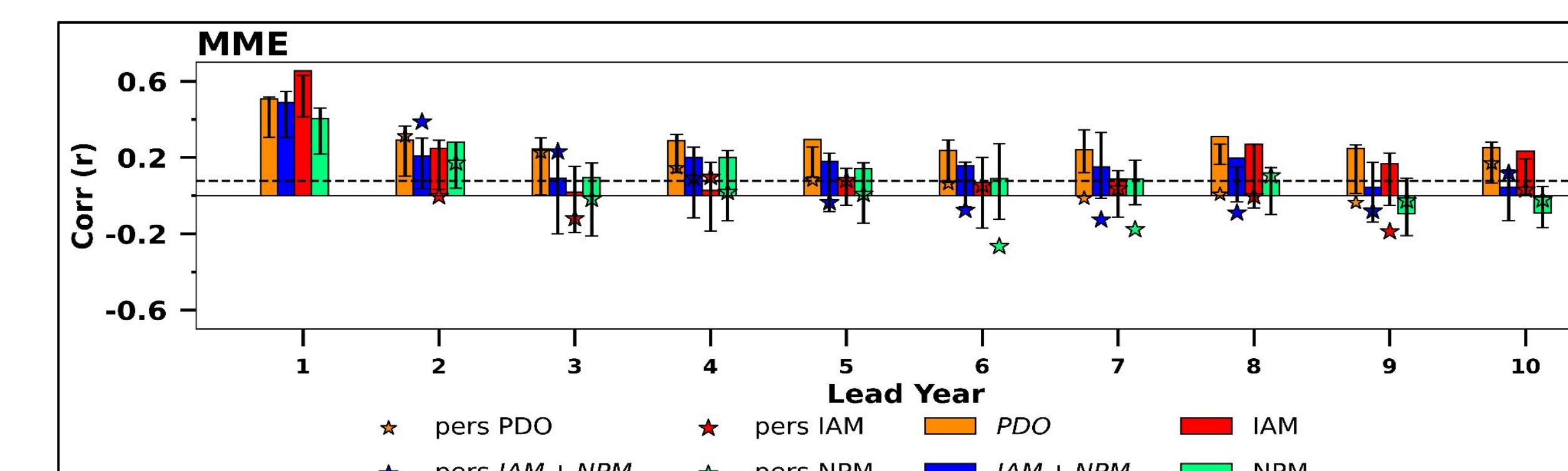
Lead time dependent SST anomaly to calculate IAM, NPM and PDO index:

$$X_{clim}(m, j, k) = \frac{1}{length(Y_i)} \sum_{Y_i} X(m, Y_i, j, k)$$

$$X_{anom}(m, j, k) = X - X_{clim}(m, j, k)$$

$m \rightarrow$  ensemble member  
 $Y_i \rightarrow$  Initialisation Year  
 $j \rightarrow$  Lead Year  
 $k \rightarrow$  Calendar month

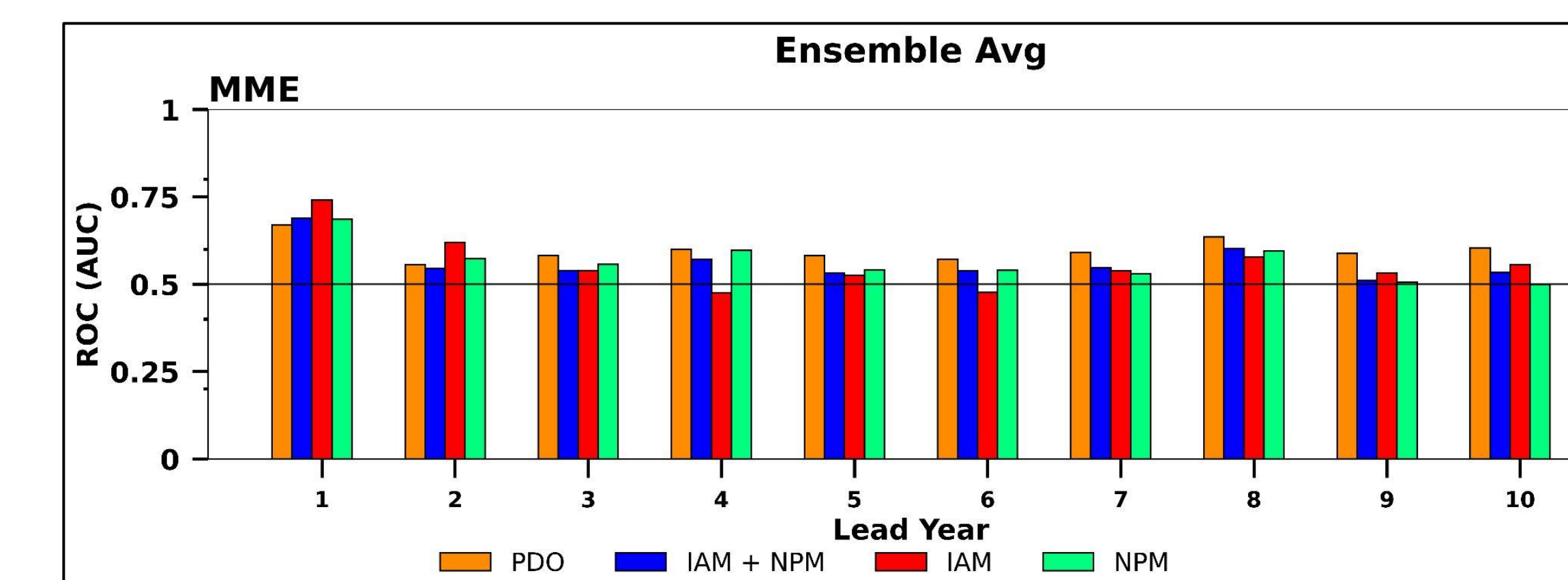
### Deterministic skill estimates:



Bars represent the ACC of respective mode of variability index in MME w.r.t. that in ERSSTv5.

Vertical black lines with whiskers represents the spread of ACC among all the models' ensemble average participating in MME.

### Probabilistic skill estimates:



For all the variability modes and almost at all the LYs, as the ROC-AUC score is above 0.5, hence MME shows some skill in predicting the phase of the variability.

## Conclusions

- All the observed variability patterns discussed in this study are well simulated in historical experiments.
- However, MME fails to reproduce the observed timescales for almost all the variability modes including PDO.
- Linear combination of IAM and NPM shares same coefficient in observation whereas in models "IAM + NPM" representing PDO like variability is biased towards NPM ( $\beta > \alpha$ )
- Despite good representation of variability patterns, models' inability to simulate NPM timescales reflects MME's inability to represent the timescales in both "IAM + NPM" and PDO.
- In phase space, unlike in observation, PDO and "IAM + NPM" calculated using equal coefficients has significant phase difference.
- From deterministic skill estimates we can infer that MME's prediction skill to predict PDO is higher than model's ability to predict "IAM + NPM" from LY2- LY10.
- PDO prediction skill is above or at par the persistence at all the lead years, whereas prediction skill of MME to predict "IAM + NPM" is below persistence at LY 2, LY3 and LY10.
- Prediction skill of MME to predict NPM drives the MME's ability to predict "IAM + NPM".

## References

- Chen, X., & Wallace, J. M. (2016). Orthogonal PDO and ENSO indices. *Journal of Climate*, 29(10), 3883-3892.
- Deser, C., & Blackmon, M. L. (1995). On the Relationship between Tropical and North Pacific Sea Surface Temperature Variations. *Journal of Climate*, 8(6), 1677-1680.